ROYAL SOCIETY OF CHEMISTRY

Journal Name

ARTICLE

Nitroxide-nitroxide and nitroxide-metal distance measurements in transition metal complexes with two or three paramagnetic centres give access to thermodynamic and kinetic stabilities

A. Giannoulis,[a, b] K. Ackermann,[a, b] P. E. Spindler,[c] C. Higgins,[b] D. B. Cordes,[b] A. M. Z. Slawin,[b] T. F. Prisner[c] and B. E. Bode[a, b]

Fundamentally, the stability of coordination complexes and of templated (bio)macromolecular assemblies depends on the thermodynamic and kinetic properties of the intermediates and final complexes formed. Here, we used pulse EPR (electron paramagnetic resonance) spectroscopy to determine the stabilities of nanoscopic assemblies formed between one or two nitroxide spin-labelled tridentate 2,2′:6′,2′′-terpyridine (tpy) ligands and divalent metal ions (Fe^{II}, Zn^{II}, Co^{II} and Cu^{II}). In three distinct approaches we exploited (a) the modulation depth of pulsed electron-electron double resonance (PELDOR) experiments in samples with increasing metal-to-ligand ratios, (b) the frequencies of PELDOR under broadband excitation using shaped pulses and (c) the distances recovered from well-resolved PELDOR data in fully deuterated samples measured at 34 GHz. The results demonstrate that PELDOR is highly sensitive to resolving the stability of templated dimers and allows to readily distinguish anti-cooperative binding (for Cu^{II} ions) from cooperative binding (for Co^{II} or Fe^{II} ions). In the case of paramagnetic ions (Co^{II} and Cu^{II}) the use of broadband PELDOR allowed to identify the cooperativity of binding from the time domain and distance data. By using a second labelled tpy ligand and by mixing two homoleptic complexes of the same metal centre we could probe the kinetic stability on a timescale of tens of seconds. Here, tpy complexes of Cu^{II} and Zn^{II} were found to be substitutionally labile, Co^{II} showed very slow exchange and Fe^{II} was inert under our conditions. Not only do our chemical models allow studying metal-ligand interactions *via* PELDOR spectroscopy, the design of our study is directly transferable to (bio)macromolecular systems for determining the kinetic and thermodynamic stabilities underpinning (templated) multimerisation. Considering the limited methods available to obtain direct information on the composition and stability of complex assemblies we believe our approach to be a valuable addition to the armoury of methods currently used to study these systems.

Introduction

(Bio)macromolecular assemblies

Macromolecular assemblies in biology and chemistry are currently at the forefront of science. They are formed by non-covalent interactions between their building blocks in a self-

[a] Biomedical Sciences Research Complex and Centre of Magnetic Resonance University of St Andrews, North Haugh, St Andrews KY16 9ST. Email: beb2@st-andrews.ac.uk

[b] EaStCHEM School of Chemistry, University of St Andrews, North Haugh, St Andrews KY16 9ST, UK

[c] Institute of Physical and Theoretical Chemistry and Center for Biomolecular Magnetic Resonance, Goethe-University Frankfurt am Main, Max-von-Laue-Str. 7, D-60438 Frankfurt am Main, Germany

organised manner and therefore possess unique properties.[1] DNA, RNA and oligomeric proteins are the best examples of self-organisation in nature. In chemical synthesis, self-assembled macromolecular architectures attract attention due to the advanced properties of the organized entities.[1, 2] One of the challenges of macromolecular assemblies is their rigorous characterisation due to their large size and extended connectivity. NMR, UV-Vis and X-ray have traditionally been applied to characterise complexes and their properties. The tridentate *2,2′:6′,2′′*-terpyridine (tpy) ligand, its derivatives and coordination complexes have played a key role in the synthesis of self-assembled (supra)molecules. Tpy-metal ion complexes exhibit unique electronic,[3-5] chemical,[6-8] optical,[3, 8, 9] photovoltaic,[10] and catalytic[6] properties and have been extensively used in medicinal chemistry,[11] materials science[12] and as catalysts.[6] Specifically, tpy-metal complexes are a vivid field of study with wide range of applications such as i) DNA intercalators,[13, 14] ii) catalysts in artificial photosynthesis,[5] in

biomimetic organic transformations and polymerizations,[6] iii) light harvesting systems,[10] iv) organic light emitting devices (OLEDs),[3] v) bio-imaging probes and sensors,[9] vi) metallo-polymers[4, 12] and the list is not exhaustive. In terms of coordination, mono- and bis-tpy complexes[15] with numerous metal ions have been reported to often form by mere mixing of the solution of ligand with a solution of the metal ion salt (Fig. 1, A).[1, 16]

In mono-tpy complexes the metal is often penta-coordinated[1] and forms a distorted trigonal bi-pyramidal geometry with solvent molecules and/or counter ions filling vacant coordination sites of the metal,[17] while in bis-tpy complexes the metal is generally hexa-coordinated and the complex is in a pseudo-octahedral geometry formed by the two ligands.[1, 18] Tpy coordination complexes are thermodynamically stable[1, 16, 18, 19] with the stabilities determined by the binding constants K_1 and K_2,[15, 18] for the mono- and bis-species, respectively (Fig. 1, A). K_1 and K_2 depend on the strength of the i) chelating effect, ii) metal-ligand electron back donation and iii) size and charge of the metal ion.[1, 16, 18] Binding can, therefore, be cooperative ($K_2 \gg K_1$), anti-cooperative ($K_2 \ll K_1$) or non-cooperative ($K_2 \approx K_1$). An interesting aspect is the dynamic nature and quick equilibration leading to the reversibility of the complex formation which can be of great importance in the design and synthesis of reversible materials.[20] The thermodynamic stability of the bis-tpy complexes with Fe^{II}, Co^{II}, Ni^{II}, Cu^{II} and Zn^{II} has been scrutinized by Dobrawa *et al.* using UV-Vis and ^1H NMR titrations as well as isothermal titration calorimetry (ITC) measurements.[21-23] Furthermore, mass spectrometry has been employed to study the stability of terpyridine binding to Cd^{II}, Co^{II}, Cu^{II}, Fe^{II}, Mn^{II}, Ni^{II} and Ru^{II} ions.[20] Recent work by some of us demonstrated that pulse EPR can monitor the formation of bis-tpy complexes using Zn^{II} ions and a spin-labelled (and thus EPR active) tpy ligand **L** ([$Zn^{II}L_2$]$^{2+}$; Fig. 1, B)[24] as well as the number of ligands **L** bound to paramagnetic Cu^{II} ions ([$Cu^{II}L_2$]$^{2+}$).[25] Here, we drive the methodology developed in reference 24 to application and study the thermodynamic and kinetic stabilities of self-assembled nanoscopic tpy complexes using Zn^{II}, Fe^{II}, Co^{II}, and Cu^{II} ions. This methodology can equally be applied to spin-labelled (bio)macromolecular assemblies for monitoring their thermodynamic and kinetic stabilities as well as different cooperativity modes.

Pulsed electron-electron double resonance spectroscopy

PELDOR (pulsed electron-electron double resonance or synonymously double electron-electron resonance, DEER) is a pulse EPR technique commonly performed at cryogenic temperatures that allows measurement of distances between unpaired electrons with angstrom resolution.[26, 27] In a nutshell, during a PELDOR experiment a set of unpaired electrons (from here on A spins) is observed using microwave pulses at a frequency ω_A, while a second set of unpaired electrons (from here on B spins) is selectively inverted by a microwave pulse at a different frequency, ω_B (Fig. 2, A). The A and B spins can be the same or different type of spin centres. If the inverted B

spins are coupled to the A spins (*i.e.* if B spins 'see' A spins) they will introduce a sudden change in the local magnetic field and resonance frequency of the A spins. Incrementing the timing t when the inversion pulse (at ω_B) is applied will lead to an increasing dephasing angle and thus a periodic modulation of the A spin signal. The periodicity of the signal will depend on the dipolar coupling frequency between A and B spins which is dependent on the A-B distance (Eq. 1).

$$v_{dip} = \frac{\mu_0 \mu_B^2 g_A g_B}{4\pi\hbar r^3}(1 - 3\cos^2\theta_{AB})$$

Eq. 1

In Eq. 1, μ_0 is the vacuum permeability μ_B is the Bohr magneton, g_A, g_B are the *g*-values of the two electron spins, $\hbar$ is the reduced Plank constant, r is the scalar distance between the two spins and θ_{AB} is the angle between the distance vector and the external magnetic field.

Here, we employed PELDOR to metal ion-tpy complexes in which the unpaired electrons reside on the metal ion (for the Cu^{II}, Co^{II} systems in Fig. 1, B, highlighted in blue) and on the nitroxide moiety (for all systems in Fig. 1, B, highlighted in red). In our distance measurements the A and B spins are either nitroxide-nitroxide or metal-nitroxide pairs.

At typical spin concentrations (~100-500 µM) used in PELDOR distance measurements, spin interactions among different complexes that yield unwanted distances (referred to as inter-molecular signal or background) interfere with the distance measurement within a single molecule (intra-molecular signal). The background signal needs to be separated from the desired dipolar coupling before determining the spin-spin distance(s). Therefore, rigorous background-correction is crucial for accurate data analysis.
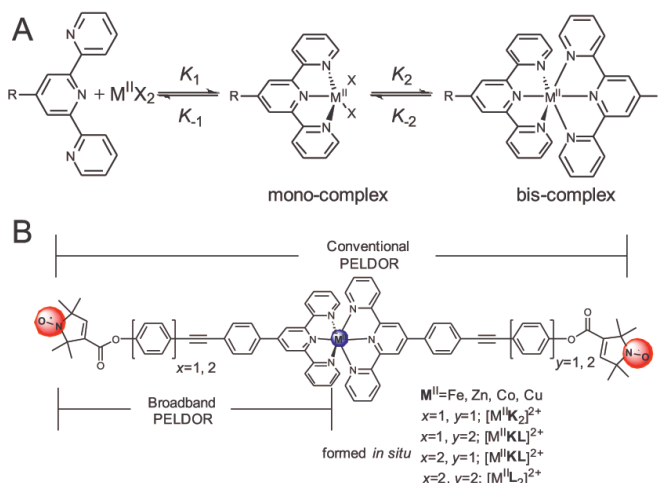

Fig. 1. A: Chemical structures of *2,2':6',2''*-terpyridine (tpy) and mono- and bis-tpy complexes formed upon addition of divalent metal ions to tpy, X represents solvent molecules or counter ions that fill the metal's coordination sphere; B: Chemical structures of the tpy-metal complexes studied with PELDOR. The relative thermodynamic stability (or cooperativity of binding) was studied with conventional PELDOR between the nitroxide-nitroxide ('pseudo-titration' series) and with broadband PELDOR between the metal-nitroxide moieties, respectively. The kinetic stability of the complexes was studied with conventional PELDOR between the nitroxide moieties in mixtures of the bis-tpy complexes with ligands **K**, **L** for a given metal ion.

After removal of the background, the data are commonly fitted to obtain a distance probability distribution. For reasons of stability, methods based on Tikhonov regularization have been established as gold standard for PELDOR data analysis.[28]

In addition to the frequencies, and therefore the distances contained in the PELDOR signal, the experiment offers further information in the form of the modulation depth, Δ, often neglected during data processing. Δ depends on the type and number of B spins inverted at ω_B and visually it is the depth of the signal on the *y*-axis of the PELDOR experiment (Fig. 2, B). It has been shown that for identical B spins Δ determines the number of spins involved in the complex or macromolecule and thus, provides information on dimerisation or multimerisation degrees.[24, 29]

Fig. 2. A: A conventional PELDOR pulse sequence for measuring spin-spin distances; B:
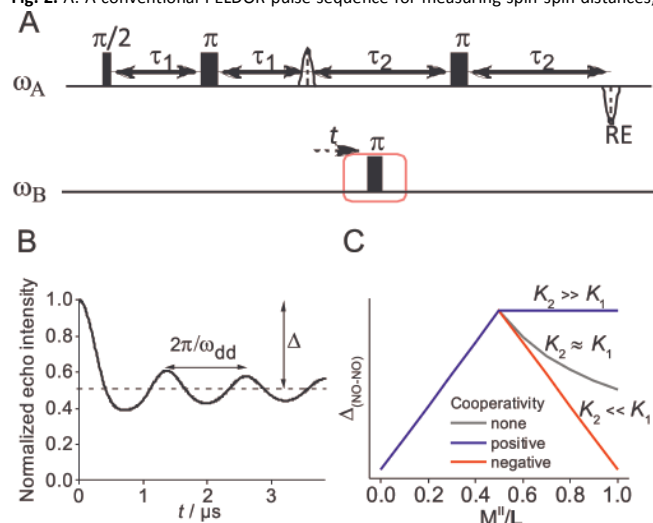
Simulated PELDOR signal that encodes i) the spin-spin distance in the spin-spin dipolar frequency, ω_{dd} and ii) the number of interacting spins in the modulation depth Δ; C: Expected trend of the PELDOR modulation depths between nitroxide spins, $\Delta_{(NO-NO)}$ *vs* increasing M^{II}/**L** ratios for different binding cooperativities of ligand **L** to the metal ion.

This work comprises three sections. In the first part, we describe the devised model of metal-tpy complexes and explain the expected trends in Δ for PELDOR experiments between the nitroxide spins for different cooperativities before comparing to experiments on Fe^{II}, Co^{II} and Cu^{II} ions.

In the second part, we explain the basis of studying the cooperativity of binding of tpy to Cu^{II} and Co^{II} complexes *via* the frequencies of the metal-nitroxide PELDOR experiment using laboratory-built instrumentation which allows inversion of the entire nitroxide EPR spectrum before comparing with experimental results.

Finally, the kinetic stabilities of all four metal-tpy complexes are scrutinised. This set of measurements exploits the distance distributions of the nitroxide-nitroxide PELDOR experiments in mixtures of metal-tpy complexes with different lengths of spin-labelled tpy ligands in order to identify kinetic stabilities with respect to ligand exchange in the range of seconds.

Results and discussion

Design of the cooperativity study and expected results

The binding of tpy to Fe^{II}, Co^{II} and Cu^{II} ions was studied by adding increasing amounts of a metal ion to a solution of ligand **L** with the M^{II}/**L** ratio ranging from 0.0 to 1.0, thereby generating a chemical model system for studying the cooperativity of binding of **L** to the three different metal centres (Fe^{II}, Co^{II}, Cu^{II}) *in situ*. The binding of **L** to Zn^{II} has been studied previously using the same protocol and was found to be neither be strongly cooperative nor anti-cooperative.[24] At M^{II}/**L** ratio 0.0 only **L** is present; by incrementing to 1.0 in steps of 0.1 different amounts of free ligand (**L**), mono-tpy complex ($[M^{II}LX_n]^{2+}$ with X representing solvent molecules or counter ions throughout the text) and bis-tpy complex ($[M^{II}L_2]^{2+}$) will be present. In practice, EPR samples were prepared as a 'pseudo-titration' series with each titration point being a different EPR sample. A ternary solvent mixture of DMSO-d_6/D$_2$O/ethylene glycol in 8/1/1 ratio with an excess of BPh_4^- as counter ion was used to ensure good solubility and avoid aggregation upon freezing.

Keeping the concentration of **L**, and thus the spin concentration, constant throughout the series allowed us to use M^{II}/**L** = 0.0 (pure solution of **L**) as experimental background for all other ratios. Of the three species potentially present and containing a nitroxide label (**L**, $[M^{II}LX_n]^{2+}$ or $[M^{II}L_2]^{2+}$) only the bis-tpy complex ($[M^{II}L_2]^{2+}$) has an intra-molecular coupled pair of nitroxides and therefore a dipolar interaction that can be measured by PELDOR spectroscopy between nitroxide spins. The free ligand **L** and the mono-complex $[M^{II}LX_n]^{2+}$ are not expected to yield any dipolar frequency and corresponding modulation depth as they do not possess any partner nitroxide spin. Therefore, the modulation depth Δ of the nitroxide-nitroxide PELDOR measurements on the 'pseudo-titration' series is expected to reflect only the amount of bis-complex $[M^{II}L_2]^{2+}$ present.

In the general case of dimerisation on a template (with M^{II} being the template) sequential addition of template to the ligand **L** will lead to the coexistence of a mixture of free monomer (**L**) and templated dimer ($[M^{II}L_2]^{2+}$) as long as there is at least a two-fold excess of monomer over the template. This assumes the binding to be strong enough to neglect competition by solvent molecules. As soon as all templates are doubly bound, *i.e.* all metals are coordinated by two **L** and dimerization is complete, addition of further template will lead to one of the three general cases: (i) the excess of free template will not dissociate the dimers $[M^{II}L_2]^{2+}$ to form mono-complexes ($[M^{II}LX_n]^{2+}$) but, instead, there will be coexistence of free template $M^{II}Cl_2$ and of bis-complex $[M^{II}L_2]^{2+}$. This will occur if the second ligand binding is thermodynamically much more stable than the first ($K_2 \gg K_1$). In this case the binding is called *cooperative*, or the cooperativity is positive; (ii) the excess of free template will dissociate the dimers $[M^{II}L_2]^{2+}$ to form mono-complexes ($[M^{II}LX_n]^{2+}$). This situation occurs when the second ligand binding is thermodynamically much less favoured than the first ($K_2 \ll K_1$) and the binding is called *anti-cooperative* or synonymously the cooperativity is negative; and (iii) the excess of free template will lead to a statistical

distribution of the ligands over the available templates and both $[M^{II}LX_n]^{2+}$, $[M^{II}L_2]^{2+}$ will coexist in solution. In this case both binding stages are thermodynamically similar ($K_2 \approx K_1$) and the binding is called non-cooperative.

For all three cooperativities, Δ will be zero at M^{II}/L = 0.0 and will linearly increase from M^{II}/L = 0.1 to 0.5. In case of cooperative binding, Δ will stay maximum for M^{II}/L ratios > 0.5 (Fig. 2, C, blue line), whereas for anti-cooperative binding Δ will linearly decrease for M^{II}/L > 0.5 (Fig. 2, C, red line). In the case of non-cooperative binding, Δ will gradually decrease at a slower rate than in the anti-cooperative case, as had been previously shown for Zn^{II} as a template.[24] The absolute value of the modulation depth Δ for a 100% bis-nitroxide system in organic solvent is expected to be 0.5 at X-band frequencies using selective pulses (length of 12 ns). However, in our models, experimental Δ values were found systematically reduced for all M^{II}/L ratios. Our deviation can be explained by incomplete labelling or the presence of orientation selection during the experiment and for this reason, we have omitted the y-axis values in the modelled Δ for the different cooperativities in Fig. 2, C. Nonetheless, the systematic Δ reduction does not interfere with reliably performing the experiment and deriving the modulation depths used to discriminate different binding modes.

Synthesis of the isolated bis-complex $[Co^{II}L_2]^{2+}$.

The syntheses and characterization of $[Fe^{II}L_2]^{2+}$, $[Zn^{II}L_2]^{2+}$, $[Cu^{II}L_2]^{2+}$ and $[Co^{II}L_2]^{2+}$ complexes have been reported by Spindler et al.[30], Ackermann et al.,[24] Meyer et al.[31] and Giannoulis et al.,[32] respectively. Additionally, we isolated and fully characterised $[Co^{II}L_2](PF_6)_2$ as a powder. This was done following standard literature protocols,[25, 31] i.e. by mixing one equivalent of $Co^{II}Cl_2$ in EtOH with two equivalents of **L** in CH_2Cl_2 followed by addition of excess of NH_4PF_6 and isolation of the complex by filtration (details and characterization in supporting information, SI). Complex formation was further verified by nitroxide-nitroxide PELDOR distance measurements (SI, Fig. S3). We then prepared the 'pseudo-titration' series samples as described in the previous section (see also the Experimental Section) and performed PELDOR experiments both detecting and inverting nitroxide spins.

Fe^{II} series. Nitroxide-nitroxide PELDOR distance measurements on the Fe^{II} 'pseudo-titration' series were performed at X-band frequencies at 50 K (Fig. 3, top). In the absence of Fe^{II} template (Fe^{II}/L ratio 0.0) the experiment features no modulation depth or oscillation as would be expected for a mono-radical (free **L**). The modulation Δ was used to monitor the bis-complex $[Fe^{II}L_2]^{2+}$ formation. Δ increased with increasing amounts of added $Fe^{II}Cl_2$ solution up to the maximum modulation depth of 0.280±0.009 at Fe^{II}/L = 0.6. For Fe^{II}/L > 0.6 Δ did not change significantly. Thus, the fraction of nitroxide in dimeric species does not decrease upon addition of excess of Fe^{II} templates and comproportionation with dissolved Fe^{II} ions to form mono-complexes is not observed. The data indicate that the binding of **L** to Fe^{II} centres is strongly cooperative. This is in accordance with Gallina et al.[19] who performed UV-Vis binding studies on a

substituted tpy ligand using $[Fe(CF_3SO_3)_2]$ in CH_2Cl_2. Furthermore, a ^1H-NMR and UV-Vis study by Dobrawa et al.[22] on a substituted tpy ligand using $[Fe(ClO_4)_2]$ in $CHCl_3/CH_3OH$ (3/2) also demonstrated the strongly cooperative binding of the tpy ligand to Fe^{II} centres. Deviation of the expected maximum Δ value from the 0.5 Fe^{II}/L ratio to 0.6 is within the experimental errors of the solutions used. This is arising from weighing small amounts (~1-2 mg) of **L** leading to uncertainties in the final concentration of the **L** solution. However, since all samples of a single series are prepared from one solution of **L** the type of cooperativity will still be reliably observed even though the equivalence point might be shifted.

In our studies, the binding mode of **L** to metal ions is based on reliably interpreting the modulation depth values over a range of M^{II}/L ratios, therefore the experimental error in Δ is important. For this reason, we have estimated the errors in Δ using two different approaches. Firstly, the background function for samples M^{II}/L > 0 was systematically varied to correspond to concentrations ranging between half and double that of the M^{II}/L = 0.0 sample concentration (determined from the experimental background function, henceforth 'bgd' method). Secondly, we assumed the background function of this reference sample (M^{II}/L = 0.0) to be identical for all other ratios. Here, the error in Δ was limited by the root-mean-square (rms) deviation between original data and fit ('rms' method). For the Fe^{II} series good agreement between Δ and errors in Δ obtained from both approaches was found.
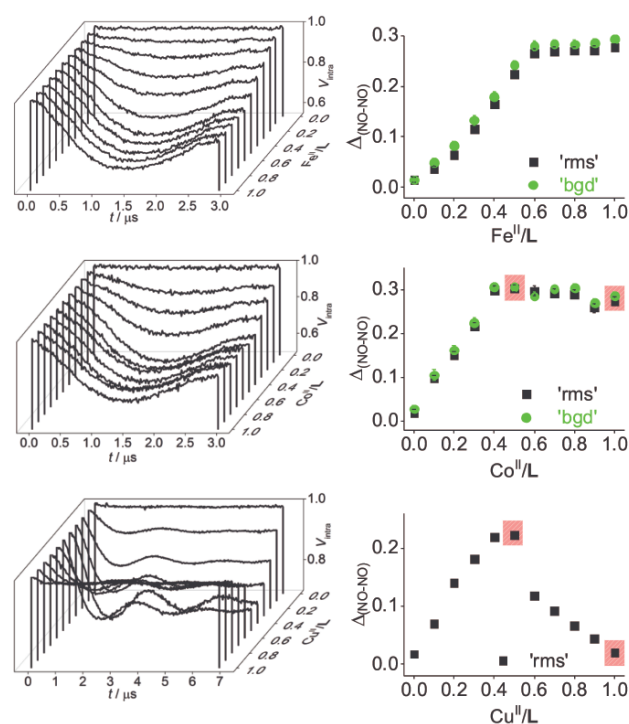

Fig. 3. Nitroxide-nitroxide PELDOR distances measurements (left) and Δ (right) vs M^{II}/L ratios 0.0 to 1.0 in 0.1 steps for Fe^{II} (top), Co^{II} (middle) and Cu^{II} (bottom) 'pseudo-titration' series. The experiment using Zn^{II} under identical experimental conditions as in the Fe^{II} series has been reported previously.[24] For Fe^{II} and Co^{II} Δ and uncertainties in Δ values were estimated with two different methods ('rms' and 'bgd', see text for details), while for Cu^{II} series the 'rms' method was sufficient due to recording of longer

PELDOR evolution times. The red shaded rectangles on the right indicate the M^{II}/**L** ratios of 0.5 and 1.0.

Co^{II} series. In contrast to diamagnetic low-spin octahedral Fe^{II} ions, low spin Co^{II} ions are paramagnetic. Fast relaxation of the Co^{II} spins at 50 K in turn enhanced the relaxation of the nitroxide spins[33-35] leading to measurements with reduced sensitivity and modulation depths. In other words, at 50 K nitroxide spin labels bound to Co^{II} relaxed faster than nitroxides present in unbound **L** molecules and therefore at this temperature free nitroxides, *i.e.* free **L**, dominated the PELDOR signal. We, therefore, reduced the measurement temperature to 10 K where Co^{II} relaxation slowed, leading to the nitroxide signals of dimeric species $[Co^{II}L_2]^{2+}$ reflecting the stoichiometry in the sample. Nitroxide-nitroxide PELDOR distance measurements as well as longitudinal and transverse relaxation measurements (termed T_1, T_m in EPR spectroscopy, respectively) of the nitroxide spins in a range of temperatures showed that 10 to 15 K are the optimum range of temperatures for performing nitroxide-nitroxide PELDOR (SI, Fig. S5). For purposes of comparison with the Cu^{II} series (see below) all nitroxide-nitroxide distance measurements of the Co^{II} series were performed at 10 K.

In the Co^{II} series, Δ gradually increased up to M^{II}/**L** ratio 0.5, as expected, indicating increasing formation of bis-complexes $[Co^{II}L_2]^{2+}$. At higher ratios, Δ stayed constant within experimental uncertainty. This means that addition of Co^{II}Cl$_2$ solution did not alter the fraction of **L** in dimers relative to free **L**. Thus, the data indicate the ligand binding to be cooperative also for cobalt. Dobrawa *et al.*[21] studied the complexation of Co^{II} by tpy using Co(ClO$_4$)$_2$·6H$_2$O in CH$_3$CN and performed ITC and UV-Vis titrations. It was found that tpy binds Co^{II} cooperatively, in agreement with our PELDOR data. As in the Fe^{II} series, the estimation of mean Δ and uncertainty in Δ was determined *via* rms deviation of the best fit or by systematic background variation with both analyses giving similar results.

Cu^{II} series. The Cu^{II}/**L** series was measured at 10 K similar to the Co^{II} series. The fast relaxation of the Cu^{II} spins at 50 K enhanced the relaxation of the nitroxide spins (SI, Fig. S7) and reduced the accessible maximum dipolar evolution times (*t*). The nitroxide-nitroxide modulation depth of ratio Cu^{II}/**L** = 0.5, as well as the T_1, T_m relaxation data of the nitroxide spins over a range of temperatures revealed 10 K to be the optimum experimental temperature for performing nitroxide-nitroxide PELDOR. The Cu^{II} and nitroxide EPR spectra overlap at 9.7 GHz (**Fig. 4**, top) making interpretation of Δ behaviour challenging at this frequency. The spectral overlap means that during a nitroxide-nitroxide PELDOR experiment not only the nitroxide spins but also the paramagnetic Cu^{II} spins (electron spin $S = 1/2$) can be excited by the microwave pulses at both frequencies, ω_A and ω_B. In this case and in combination with the low measurement temperatures (10 K) Cu^{II} spins are expected to contribute significantly during the nitroxide-nitroxide PELDOR experiment making interpretation of modulation depth values dependent on the Cu^{II} contribution to both the signal strength and the modulation depth. The reliable extraction of the nitroxide-nitroxide modulation depths from overlapping spectra is under investigation and will be reported elsewhere. Therefore, in contrast to the Fe^{II} and

Co^{II} series that were performed at X-band frequencies (9.7 GHz), the nitroxide-nitroxide PELDOR measurements on the Cu^{II} series were performed at Q-band frequencies (34 GHz) where Cu^{II} and nitroxide spins are spectrally well separated (Fig. 4, bottom).

The higher sensitivity of the Q-band spectrometer allowed recording up to a *t* of 7 μs in a reasonable amount of measurement time (~1.5-3.0 h) in contrast to the previously used 3 μs for the Fe^{II} and Co^{II} series (requiring ~1-3 h at X-band). Here, the reliability in the background removal increased due to the recording of increased maximum *t* and therefore, the Cu^{II}/**L** ratio of 0.0 was used only as an indication of the background function while the best fit was employed for the experimental determination with the 'rms' method. Determination of Δ with the 'bgd' method was unfeasible due the background being confined to a much smaller range by the increased maximum *t*. As expected, Δ increased up to ratio 0.5 indicating an increase of the $[Cu^{II}L_2]^{2+}$ complexes formed upon addition of Cu^{II}Cl$_2$, while after that ratio Δ decreased gradually. The decrease in Δ demonstrates dissociation of bis-complex $[Cu^{II}L_2]^{2+}$ due to excess template to yield mono-complexes $[Cu^{II}LX_n]^{2+}$, *i.e.* a single tpy ligand **L** bound to Cu^{II}. Following the steepness of the decline, **L** binding to Cu^{II} was found to be anti-cooperative (Fig. 3, bottom). The complexation of Cu^{II} ions by tpy was previously studied using ITC and UV-Vis titrations by Dobrawa *et al.*[21] where indeed anti-cooperative binding of tpy to Cu^{II} ions using Cu(ClO$_4$)$_2$·6H$_2$O in CH$_3$CN was reported, in agreement with our PELDOR data.
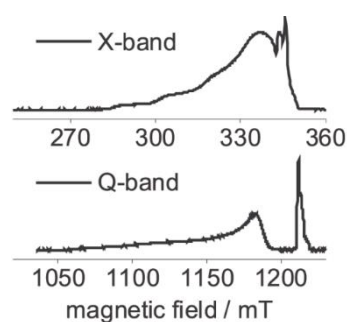

Fig. 4. Field-swept spectra of Cu^{II}/**L** ratio 0.5 optimized for the Cu^{II} spins measured at X-(top) and Q-band (bottom) frequencies at 10 K.

Broadband metal-nitroxide PELDOR distance measurements

Design of the broadband study and expected results

Studying the metal-ligand binding by nitroxide-nitroxide PELDOR titrations might not always be feasible. Especially the presence of free spin label or incomplete labelling will make the quantification of modulation depths less reliable than in our models. Therefore, a different approach that would allow identifying the mere presence of templated dimers would be valuable in studying the cooperativity of binding.

In our chemical models M^{II}-nitroxide PELDOR measurements with nitroxides acting as B spins are expected to reveal only minor Δ differences, therefore making a distinction of different binding cooperativities challenging.

Additionally, modelled Δ values in M^{II}-nitroxide PELDOR titrations in systems where the metal amount stays constant and increasing amounts of **L** are added revealed the approach not to be sensitive in probing different cooperativities (modelled Δ values are shown in SI, Fig. S9).

Therefore, we did not pursue any such approach for distinguishing cooperativities. Instead, we tested whether the presence and absence of combination frequencies can be used to identify different cooperativity regimes.

It is well-established in PELDOR applications that participation of more than two spins during the experiment, *i.e.* if more than one spin per complex is inverted at ω_B, this can give rise to multi-spin effects.[36-41] These effects manifest in the PELDOR experiment by appearance of unwanted frequencies or the 'quenching' of wanted dipolar frequencies by broadening. The effect on the PELDOR data depends on the number of B spins and their inversion efficiency at ω_B.[36, 40] These effects, in turn, yield additional peaks or diminish wanted distances in the distance distributions obtained by Tikhonov regularization procedures where the data is analysed with a two-spin kernel function. The effects scale with an increasing number of inverted B spins. A large B spin inversion probability can yield significant multi-spin effects already in a three-spin system. This can be deliberately exploited by using pulses with a spectrally broader inversion profile than common rectangular pulses, *i.e.* by substituting the π pulse at ω_B by a 'shaped' or 'broadband' pulse (*e.g.* wideband uniform rate smooth truncation, WURST, or chirp pulse).[30, 42-50] A similar purpose can be pursued by using phase modulated (composite) pulses.[46] Both, amplitude and phase modulated pulses yield enhanced signal-to-noise ratios and Δ, when compared to rectangular pulses.[30, 44, 46, 48-51]

In our models, the Co^{II} and Cu^{II} ions are EPR active (with electronic spin $S = 1/2$). In this set of experiments, we employed Co^{II}-nitroxide and Cu^{II}-nitroxide PELDOR distance measurements using broadband B spin inversion on the 0.5 and 1.0 M^{II}/**L** ratios.

In our measurements the metal ion centred spin was observed at ω_A (A spin) and the nitroxide spins were inverted at ω_B (B spins) using a WURST pulse as inversion pulse. It is anticipated that in three-spin systems WURST PELDOR will yield an additional frequency in the PELDOR time domain data and therefore, the so-called 'ghost' peak is expected to appear in the distance domain after Tikhonov regularization. From the 'pseudo-titration' series data it was found that at 0.5 M^{II}/**L** ratio both metal complexes are in the form $[M^{II}L_2]^{2+}$ and therefore are three-spin systems (one metal spin and two nitroxide spins per complex).

Thus, for both Co^{II} and Cu^{II} complexes at M^{II}/**L** = 0.5 WURST PELDOR is expected to display three-spin effects and the 'ghost' peak. The Co^{II} complex displayed cooperative binding and, therefore, at Co^{II}/**L** = 1.0 a three-spin system ($[Co^{II}L_2]^{2+}$) will coexist with solvated Co^{II} ions, expected to yield the 'ghost' peak upon broadband nitroxide spin inversion. On the contrary, the Cu^{II} complex exhibited anti-cooperative binding and at Cu^{II}/**L** = 1.0 Cu^{II} is expected to form mono-tpy

complexes ($[Cu^{II}LX_n]^{2+}$) being two-spin systems which should not yield any 'ghost' peak in WURST PELDOR.

Therefore, the hypothesis is that the different binding cooperativities and the presence of three spins in general are distinguishable using the frequencies of the PELDOR experiment rather than Δ. The dipolar frequency of the 'ghost' peak should be double of that of the wanted dipolar coupling.[39] From the X-ray structure of **L**[24] and existing metal ion-tpy structures we expect the metal-nitroxide distance to be ~2.6 nm[31] (corresponding to a dipolar coupling of ~2.9 MHz). This, in turn, means the 'ghost peak should appear at 2.0 nm corresponding to a dipolar coupling of ~5.8 MHz.

Co^{II}-nitroxide WURST PELDOR

Although the Co^{II} system in the ternary solvent mixture of DMSO-d_6/D_2O/ethylene glycol had previously been shown to have favourable EPR properties at W-Band (94 GHz)[32] this was not reproducibly achieved for the present X-band study. The T_1 and T_m relaxation rates of the Co^{II} spins were very fast making it difficult to detect Co^{II} rendering Co^{II}-nitroxide distance measurements unfeasible. Therefore, the Co^{II}-nitroxide WURST PELDOR measurements were performed in a different solvent system than the Co^{II} series for Δ. Co^{II} relaxation significantly improved when the samples were prepared under an inert atmosphere of Ar using dry DMF/toluene 1/9 and a very weakly coordinating anion, $BAr^F_4{}^-$, instead of $BPh_4{}^-$.[17]

These conditions allowed performing Co^{II}-nitroxide distance measurements (Fig. 5, top).

The distance distributions of the Co^{II}-nitroxide WURST PELDOR measurements on both 0.5 and 1.0 Co^{II}/**L** ratios reveal the expected Co^{II}-nitroxide distance at 2.6 nm, as well as the 'ghost' peak at 2.0 nm. The position of the 'ghost' peak is in perfect agreement with the expected double frequency as discussed above.
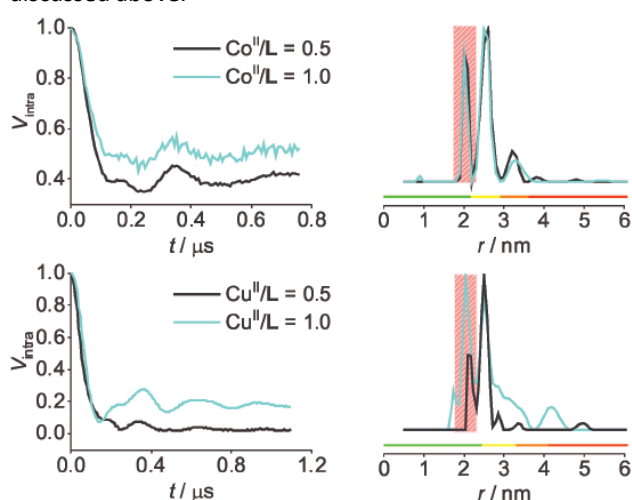

Fig. 5. Background corrected metal-nitroxide PELDOR data (left) and corresponding distance distributions (right) of the 0.5 and 1.0 Co^{II}/**L** (top) and Cu^{II}/**L** (bottom) ratios measured with WURST inversion pulse at X-band frequencies. Traces and distance probability distributions for M^{II}/**L** =0.5 and 1.0 in black and light blue, respectively. The expected 'ghost' at 2.0 nm is highlighted by the red shaded areas. The colour coding in the distance distribution indicates reliability with reliable distribution shape (green), reliable mean and width (yellow) and reliable mean only (amber). Intensity in the red indicates the presence of long distances that are not quantifiable.

The appearance of the 'ghost' peak at the 1.0 Co^{II}/**L** ratio demonstrates the presence of the third spin and deductively the presence of the $[Co^{II}L_2]^{2+}$ complex with two equivalents of **L** with respect to the Co^{II} ion. The 'ghost' and the wanted peaks for both Co^{II}/**L** ratios persisted with statistical analyses of the distance distributions upon introduction of experimental noise and Monte Carlo variation of the background function as well as upon a post-processing procedure referred as 'power scaling' that diminishes multi-spin effects ('validated' distance distributions before and after 'power scaling' in SI, Fig. S12). Thus, the broadband Co^{II}-nitroxide PELDOR supports the cooperative binding of the tpy moiety to Co^{II} ions found from the 'pseudo-titration' series.

Cu^{II}-nitroxide WURST PELDOR

The Cu^{II}-nitroxide WURST PELDOR measurements of complexes with Cu^{II}/**L** 0.5 and 1.0 were performed in the same solvent mixture as the Cu^{II} 'pseudo-titration' series displaying reasonable relaxation properties of the Cu^{II} spins. The corresponding distance distributions feature the Cu^{II}-nitroxide distance at 2.6 nm. Furthermore, the distance distribution of Cu^{II}/**L** = 0.5 displays the 'ghost' peak at 2.0 nm as would be expected for a three-spin system. The distance distribution of Cu^{II}/**L** = 1.0 complex features a smaller intensity and slightly shifted peak from the 'ghost' peak of the Co^{II}/**L** ratio 0.5 present at 2.1 nm. Even with complete suppression of combination frequencies similar complexes studied previously by Narr *et al.*[52] and Meyer *et al.*[31] have shown orientation selection leading to an increased contribution of the double frequency which in our system coincides with the frequency (and thus apparent distance) of the 'ghost' peak. The presence of orientation selection in the Cu^{II}-nitroxide measurement was also tested in our system (SI, Fig. S16) where the distance distribution of the Cu^{II}-nitroxide measurement with rectangular inversion pulse has the peak at 2.1 nm present, while this peak is absent from the corresponding Co^{II}-nitroxide distance measurement (SI, Fig. S13). Since no three-spin effects and corresponding 'ghost' peaks are observed in our PELDOR experiments with rectangular pulses, the residual peak at 2.1 nm in the broadband Cu^{II}-nitroxide measurement of ratio 1.0 can be attributed to orientation selection as has been predicted from the Cu^{II}-tpy *g*-tensor.[53] For the 1.0 ratio statistical analyses of the distance distributions obtained upon introduction of experimental noise and Monte Carlo variation of the background function and upon 'power scaling' showed that both peaks persist (SI, Fig. S15). No such analysis could be performed for the 0.5 ratio due to the large Δ of this measurement making power-scaling unfeasible and background correction unreliable.

Ligand exchange ('scrambling') experiments

In a final set of experiments the kinetic stability of the $[M^{II}L_2]^{2+}$ complexes of Zn^{II}, Fe^{II}, Co^{II} and Cu^{II} was assessed semi-quantitatively during the time scale of sample preparation (~30 s). To this end, we devised a new model where two different *in situ* formed bis-complexes (*i.e.* 0.5 M^{II}/ligand ratio)
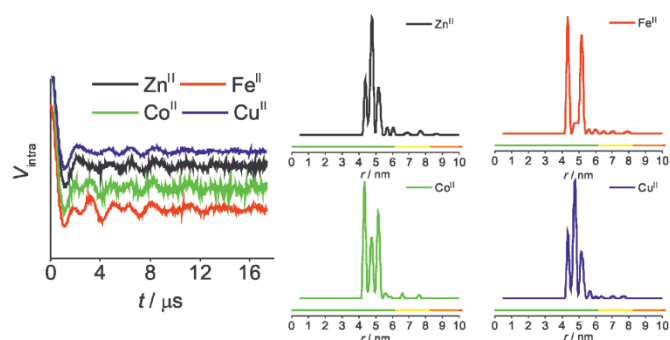

Fig. 6. Background corrected nitroxide-nitroxide PELDOR data (left, the traces are shown with an offset on the *y*-axis for better visualisation) and corresponding distance distributions (right) of the mixtures of the bis-complexes of Zn^{II}, Fe^{II}, Co^{II} and Cu^{II} with tpys **K** and **L**. See Fig. for the meaning of the reliability colour bars.

for a given metal ion were mixed with each other. The synthesis of novel spin-labelled terpyridine ligand **K** (details in SI) was analogous to the previously published synthesis of **L**.[24] The bis-complexes of all four metal centres with two spin-labelled tpy ligands **K** and **L** that differed only in their lengths were prepared *in situ*, followed by mixing of the two solutions for 5 s and sample transfer into quartz tubes and immediate freezing in liquid nitrogen (~25 s). Each bis-complex, *i.e.* $[M^{II}L_2]^{2+}$ and $[M^{II}K_2]^{2+}$ (Fig. 1, B; $x = y = 2$ and $x = y = 1$, respectively) is expected to have a distinct nitroxide-distance peak when performing nitroxide-nitroxide PELDOR with rectangular inversion pulse (Fig. 2, A). Based on the crystal structures of **K** (SI, Scheme S1) and **L**[24] the respective nitroxide-nitroxide distances of 5.2 and 4.3 nm are expected for $[M^{II}L_2]$ and $[M^{II}K_2]$. If **K**, **L** exchange during mixing of the distinct bis-complexes then a third peak at ~4.8 nm corresponding to the mixed $[M^{II}KL]^{2+}$ complex should appear in the distance distribution of the nitroxide-nitroxide PELDOR distance measurement. The presence or absence of this peak is expected to inform on the kinetic stabilities of the bis-complexes in the time scale of sample preparation, *i.e.* whether measurable ligand exchange (scrambling) has taken place.

In detail, if upon mixing of the $[M^{II}L_2]$ and $[M^{II}K_2]$ complexes for a given metal ion there is no ligand exchange, as would be expected for substitutionally inert complexes, the distance distribution should feature only the 4.3 nm and 5.2 nm peaks corresponding to the nitroxide-nitroxide distances of the constituting complexes (Fig. 1, B). If the complexes formed are substitutionally labile, the ligand composition of the two complexes will be scrambled therefore, in addition to the 4.3 and 5.2 nm peaks of the original bis-complexes a third peak corresponding to the mixed $[M^{II}KL]^{2+}$ complex (Fig. 1, B) should appear in the distance distribution. In this case, the peak ratios (short/mixed/long) should correspond to the binomial coefficients (1/2/1) upon completion of ligand scrambling to equilibrium. In the approximation that the lower K_2 in non- and anti-cooperative binding behaviour is dominated by the ligand dissociation rate, ligand scrambling and the presence of the third peak can be expected in the non-cooperative and anti-cooperative systems (*i.e.* for the Zn^{II} and Cu^{II} ions, respectively). The nitroxide-nitroxide PELDOR distance

measurements of the mixtures of the bis-complexes of Zn^{II}, Fe^{II}, Co^{II} and Cu^{II} ions with tpys **K** and **L** using rectangular inversion pulse at ω_B are shown in Fig. 6. The distance distribution of the mixed $[Zn^{II}K_2]^{2+}$ and $[Zn^{II}L_2]^{2+}$ complexes features three peaks. The peaks at 4.3 nm and 5.2 nm correspond to the bis-complexes of Zn^{II} with **K** and **L** respectively, while the peak at 4.8 nm corresponds to the mixed $[Zn^{II}KL]^{2+}$ complex. The double intensity of the middle peak reflects the double-fold concentration of the mixed complex with respect to the remaining $[Zn^{II}K_2]$ and $[Zn^{II}L_2]$ complexes, as it would be expected for a fully scrambled system. The ligand scrambling experiment, thus, shows that in the timescale of the sample preparation the ligands exchange to a purely statistical mixture. The distance distribution of the mixed $[Fe^{II}K_2]^{2+}$ and $[Fe^{II}L_2]^{2+}$ complexes exhibits two peaks, corresponding to the non-exchanged starting complexes. No middle peak is present meaning that the complexes are kinetically highly stable on the timescale of the sample preparation and the ligands do not scramble to form the mixed complex. This kinetic experiment is consistent with the strongly cooperative binding of the tpy moiety to Fe^{II} ion as shown earlier with the 'pseudo-titration' experiment. The distance distribution of the mixed $[Co^{II}K_2]^{2+}$ and $[Co^{II}L_2]^{2+}$ complexes exhibits three peaks corresponding to all three possible (short, mixed, long) nitroxide-nitroxide distances. However, the middle peak does not have the double intensity as in the case of the experiment with Zn^{II}. The data suggests that ligand exchange has taken place but has not yet reached equilibrium on the time scale of the sample preparation. However, the emergence of the middle peak shows that the Co^{II} complexes are kinetically less stable than their iron analogues. On the other hand, the cooperativity of **L** binding to Co^{II} was found to be positive, indicating high thermodynamic stability of the bis-complex. Nitroxide-nitroxide PELDOR distance measurements of the mixed $[Cu^{II}K_2]^{2+}$ and $[Cu^{II}L_2]^{2+}$ complexes revealed three peaks in the distance distribution in 1/2/1 ratio, as in the case of the Zn^{II} mixtures. The appearance of the middle peak shows that the $[Cu^{II}K_2]^{2+}$ and $[Cu^{II}L_2]^{2+}$ complexes are not kinetically stable. Although non-cooperative and anti-cooperative systems cannot be distinguished by our ligand exchange experiments, the presence of the middle peak in the Cu^{II} system corresponding to the mixed complex supports the quick dissociation of the second tpy and the high kinetic instability of the Cu^{II} complexes. Overall, our results are in good agreement with ligand exchange data based on ^3H labelled tpy by Hogg and Wilkins[54] where it was found that for the Cu^{II} and Zn^{II} ions the exchange of tpy ligands is too rapid to obtain kinetic data, while the ligand exchange for Fe^{II} is very slow (half-life of 140 h at 35.4°C).[54] In the case of Co^{II}, kinetic data could be obtained. Indicatively, in the bis-tpy Co^{II} complex the ligand exchange proceeds with a half-life of 36 min at 10.5 °C,[54] however, no room temperature exchange data are reported for the Co^{II} ion. The results are also in perfect agreement with the stabilities of octahedral complexes expected from crystal field theory. Here the stabilisation energy is expected maximum for low-spin Fe^{II} and reduces via Co^{II} and Cu^{II} to zero at Zn^{II}. With this set of experiments, we

have shown that PELDOR spectroscopy can provide insights on kinetic stabilities of metal-tpy complexes. A detailed kinetic study of the Zn^{II} and Cu^{II} systems would require rapid freeze quench techniques which allow second to millisecond dissection of the binding process followed by PELDOR measurements. However, these types of measurements are outside the scope of this work. For the Co^{II} ion mixing of the $[Co^{II}K_2]^{2+}$ and $[Co^{II}L_2]^{2+}$ complexes with increasing time scales before freezing the mixtures is particularly interesting and will be reported in due course.

It is important to mention that we can reliably distinguish three close-by peaks and reliably interpret the data due to recording of sufficiently long PELDOR evolution times. Therefore, for such type of experiments one should aim for extended PELDOR time evolution windows.[55]

The PELDOR data for each metal ion are shown in the SI, Fig. S21 and statistical variation of the background removal and introduction of noise demonstrate that the obtained peaks persist (SI, Fig. S22).

Conclusions

PELDOR spectroscopy was employed to assess the cooperativity of binding of tpy ligand **L** to 3d metal ions. Three different cooperativity modes (non-cooperative,[24] cooperative, and anti-cooperative) could be probed by the modulation depth Δ of PELDOR 'pseudo-titration' experiments exploiting the nitroxide spin labels in **L**. In the case of Co^{II} and Cu^{II} ions, the cooperativity mode was additionally identified *via* the frequencies of broadband metal ion-nitroxide PELDOR experiments. The presence and absence of the 'ghost' peak in the distance distribution of the equimolar Co^{II}/**L** and Cu^{II}/**L** mixtures, respectively, confirmed the cooperative and anti-cooperative binding as found from the modulation depth data. The broadband experiments can prove advantageous in applications where Δ is difficult to quantify. We further studied the tpy ligand exchange for all metal ions semi-quantitatively on a half-minute time scale. This was done by analysis of the distance distributions in mixtures of $[M^{II}K_2]^{2+}$ and $[M^{II}L_2]^{2+}$. Bis-tpy complexes of Zn^{II} and Cu^{II} were labile, Fe^{II} was inert whereas Co^{II} showed some slow ligand exchange but did not reach equilibrium on the time-scale investigated. Even though these experiments provide only a rough estimate on the kinetic stabilities of the metal bis-tpy complexes they open up new possibilities for studying kinetics in coordination complexes. Additionally, our results on tpy complexes with Fe^{II}, Zn^{II}, Co^{II} and Cu^{II} ions provide a better understanding of tpy-metal interactions and complement and support existing data. Overall, we demonstrated the potential of studying metal-ligand interactions by performing nanometer range distance measurements. This work showcases three experimental approaches for studying thermodynamic and kinetic stabilities of (bio)macromolecular assemblies whose investigation by conventional techniques such as NMR is challenging.

Experimental section

EPR sample preparation

The M^{II}/**L** ratios of the 'pseudo-titration' series were prepared *in situ* by mixing a solution of **L** in CH_2Cl_2 (50 µL, 200 µM) with $M^{II}Cl_2$ solution in EtOH (0 to 50 µL, 200 µM). The solution was mixed for 30 s and the solvents were evaporated *in vacuo*. The residue was re-dissolved in DMSO-d_6/D_2O/ethylene glycol (8/1/1) to reach a final volume of 100 µL and $NaBPh_4$ was added in at least ten-fold excess. The samples for testing ligand scrambling/exchange were prepared *in situ* by individually mixing a solution of **L** in CH_2Cl_2 (50 µL, 200 µM) with $M^{II}Cl_2$ solution in EtOH (25 µL, 200 µM) and a solution of **K** in CH_2Cl_2 (50 µL, 200 µM) with $M^{II}Cl_2$ solution in EtOH (25 µL, 200 µM). Each solution was individually mixed for 30 s and evaporated *in vacuo*. The residues were re-dissolved in DMSO-d_6/D_2O/ethylene glycol-d_6 (8/1/1, 100 µL) after addition of ten-fold excess or more of $NaBPh_4$. 50 µL of each of the resulting solutions were mixed with each other for 5 s before rapid sample transfer and freezing in liquid nitrogen (~25 s). For X-band measurements each solution (100 µL) was transferred to a 4 mm quartz EPR tube, while for Q-band measurements, 70 µL of the solution was transferred to a 3 mm quartz EPR tube.

EPR instrumentation and collection of data

PELDOR data were recorded on an ELEXSYS E580 pulsed X-band (~9.7 GHz) or Q-band (~34.0 GHz) EPR spectrometer including the second frequency option (E580-400U) from Bruker. Pulses were amplified by travelling wave tube (TWT) amplifiers (1 kW at X-band and 150 W at Q-band) from Applied Systems Engineering. An MD5 dielectric ring resonator (X-band) and a TE012 cavity (Q-band) with standard flex line probe heads were used. The established 4-pulse PELDOR $\pi/2(\nu_A) - \tau_1 - \pi(\nu_A) - (\tau_1 + t) - \pi(\nu_B) - (\tau_2 - t) - \pi(\nu_A) - \tau_2$ —echo [56] pulse sequence was employed. For all nitroxide-nitroxide PELDOR measurements of the 'pseudo-titration' series at Q-band the pump pulse was set to 14 ns, while for measurements in MD5 resonator at X-band the inversion pulse length was set either to 18 or 20 ns. All nitroxide-nitroxide PELDOR measurements of the Cu^{II} and Co^{II} complexes were acquired at 10 K, using a shot repetition time of 150 ms, while measurements of the Fe^{II} complexes were acquired at 50 K with a shot repetition time of 3 ms. τ_1 was set to 380 ns and τ_2 to 3.12 µs for all 'pseudo-titration' series measurements apart from the Cu^{II} series at Q-band where τ_2 was set to 7 µs. In all measurements, the pump pulse was set to the maximum of the nitroxide spectrum while the detection sequence was applied at 70 MHz higher frequency for X-band and 80 MHz lower frequency for Q-band measurements. Ligand scrambling experiments on Cu^{II} and Co^{II} complexes were recorded at 20 K with a shot repetition time of 50 ms, while on Zn^{II} and Fe^{II} at 50 K with a shot repetition time of 3 ms. For all measurements the inversion pulse was set to 12 ns, τ_1 to 760 ns and τ_2 to 20 µs. Cu^{II}-nitroxide and Co^{II}-nitroxide measurements were recorded in an MS3 resonator at X-band with rectangular and broadband pulses. For all measurements the inversion pulse was set to the maximum of the nitroxide spectrum while the detection sequence was set to 180 MHz lower frequency for rectangular inversion pulse PELDOR and 280 MHz lower frequency for WURST inversion pulse PELDOR. All measurements with rectangular pulses were recorded at 15 K with a shot repetition time of 1.5 ms and an inversion pulse of 12 ns. τ_1 was set to 380 ns for both Cu^{II} and Co^{II} samples, while τ_2 was set to 2.36 µs for the Cu^{II} complex and to 1.94 µs for the Co^{II} complex. Broadband measurements of the Cu^{II} complex were run at 10 K with a shot repetition time of 2.4 ms, while the broadband measurements of Co^{II} were run at 4 K with a shot repetition time of 1.6 ms. The τ_1 of both the Cu^{II} samples was set to 400 ns and τ_2 was set to 1.2 µs for the 0.5 Cu^{II}/**L** ratio and to 2.4 for the 1.0 Cu^{II}/**L** ratio. The τ_1 and τ_2 values for both Co^{II} systems were set to 360 ns and 960 ns, respectively.

Data processing

The nitroxide-nitroxide ('pseudo-titration' series and ligand exchange experiments) and metal-nitroxide PELDOR data were analysed with the DeerAnalysis2015 program (DA). The distance distributions were obtained by Tikhonov regularization using the L-curve criterion. In the M^{II}/**L** series the 0.0 ratio was used to experimentally extract the background function. During this processing, the modulation depth values are the output values of DeerAnalysis program corresponding to the best fit of the trace to the experimental data, Δ and rms$_\Delta$ ('rms' method). Additionally, the modulation depths and standard deviations (Δ and SD$_\Delta$) have been calculated upon variation of the background to values that correspond between half and double the density of the 0.0 ratio ('bgd' method).

Due to noise in the primary data and uncertainties in the extraction of the background we performed validations of the distance distributions in the broadband metal-nitroxide and ligand exchange experiments series within the validation tool of DeerAnalysis2015. This tool allows performing statistical error analysis considering different levels of noise and different background corrections by varying the local concentration in a Monte Carlo fashion. During this procedure, the mean distance probability and the standard deviation for each point were obtained. Statistical variation of the background was performed with a background start from 5% to 80% of the time window and 16 trials (every 5%) and white noise of a level 1.50 and 50 trials, followed by pruning level of 1.15 (*i.e.* retaining the data sets exceeding the lowest RMSD by a maximum of 15%). If less than 50% of trials were retained upon pruning, the traces were cut by 10% (and up to 30% percent) until half or more of the trials were within 15% of the lowest RMSD. The colour coded reliability bars in Fig. 5, Fig. 6 and in some of the figures in SI are according to reference.[28]

Conflicts of interest

There are no conflicts of interest to declare.

Acknowledgements

Notes and references

1. H. Hofmeier and U. S. Schubert, *Chem. Soc. Rev.*, 2004, **33**, 373-399.
2. J. Veliks, J. C. Tseng, K. I. Arias, F. Weisshar, A. Linden and J. S. Siegel, *Chem. Sci.*, 2014, **5**, 4317-4327.
3. H. Sasabe, Y. Hayasaka, R. Komatsu, K. Nakao and J. Kido, *Chem. - Eur. J.*, 2017, **23**, 114-119.
4. O. Kotova, R. Daly, C. M. G. dos Santos, M. Boese, P. E. Kruger, J. J. Boland and T. Gunnlaugsson, *Angew. Chem. Int. Edit. Engl.*, 2012, **51**, 7208-7212.
5. L. Favereau, A. Makhal, D. Provost, Y. Pellegrin, E. Blart, E. Goransson, L. Hammarstrom and F. Odobel, *Phys. Chem. Chem. Phys.*, 2017, **19**, 4778-4786.
6. A. Winter, G. R. Newkome and U. S. Schubert, *Chemcatchem*, 2011, **3**, 1384-1406.
7. A. Winter, A. M. J. van den Berg, R. Hoogenboom, G. Kickelbick and U. S. Schubert, *Synthesis*, 2006, **17**, 2873-2878.
8. D. F. Wu, T. Shao, J. Men, X. C. Chen and G. W. Gao, *Dalton Trans.*, 2014, **43**, 1753-1761.
9. Q. Zhang, X. H. Tian, Z. J. Hu, C. Brommesson, J. Y. Wu, H. P. Zhou, S. L. Li, J. X. Yang, Z. Q. Sun, Y. P. Tian and K. Uvdal, *J. Mater. Chem. B*, 2015, **3**, 7213-7221.
10. D. Saccone, C. Magistris, N. Barbero, P. Quagliotto, C. Barolo and G. Viscardi, *Materials*, 2016, **9**, 1-37.
11. A. Winter, M. Gottschaldt, G. R. Newkome and U. S. Schubert, *Curr. Top. Med. Chem.*, 2012, **12**, 158-175.
12. B. G. G. Lohmeijer and U. S. Schubert, *Angew. Chem. Int. Edit. Engl.*, 2002, **41**, 3825-3829.
13. D. Lazic, A. Arsenijevic, R. Puchta, Z. D. Bugarcic and A. Rilak, *Dalton Trans.*, 2016, **45**, 4633-4646.
14. M. M. Milutinovic, A. Rilak, I. Bratsos, O. Klisuric, M. Vranes, N. Gligorijevic, S. Radulovic and Z. D. Bugarcic, *J. Inorg. Biochem.*, 2017, **169**, 1-12.
15. R. H. Holyer, C. D. Hubbard, S. F. A. Kettle and R. G. Wilkins, *Inorg. Chem.*, 1966, **5**, 622-625.
16. A. Winter, C. Friebe, M. D. Hager and U. S. Schubert, *Eur. J. Org. Chem.*, 2009, 801-809.
17. R. Diaz-Torres and S. Alvarez, *Dalton Trans.*, 2011, **40**, 10742-10750.
18. U. S. Schubert, H. Hofmeier and G. R. Newkome, in *Modern Terpyridine Chemistry*, Wiley-VCH Verlag GmbH & Co. KGaA, Weinheim, Germany, 2006, pp. 7-35.
19. M. E. Gallina, G. Bergamini, S. Di Motta, J. Sakamoto, F. Negri and P. Ceroni, *Photochem. Photobiol. Sci.*, 2014, **13**, 997-1004.
20. M. A. R. Meier, B. G. G. Lohmeijer and U. S. Schubert, *J. Mass Spectrom.*, 2003, **38**, 510-516.
21. R. Dobrawa, P. Ballester, C. R. Saha-Moller and F. Wurthner, in *Metal-containing and metallosupramolecular polymers and materials*, ed. U. S. Schubert, G. R. Newkome and I. Manners, American Chemical Society, 2006, vol. 928, pp. 43-62.
22. R. Dobrawa and F. Wurthner, *Chem. Commun.*, 2002, 1878-1879.
23. R. Dobrawa and F. Wurthner, *J. Polym. Sci., Part A: Polym. Chem.*, 2005, **43**, 4981-4995.
24. K. Ackermann, A. Giannoulis, D. B. Cordes, A. M. Z. Slawin and B. E. Bode, *Chem. Commun.*, 2015, **51**, 5257-5260.
25. A. Giannoulis, M. Oranges and B. E. Bode, *ChemPhysChem*, 2017, **18**, 2318-2321.
26. R. E. Martin, M. Pannier, F. Diederich, V. Gramlich, M. Hubrich and H. W. Spiess, *Angew. Chem. Int. Ed. Engl.*, 1998, **37**, 2834-2837.
27. A. D. Milov, K. M. Salikhov and M. D. Shirov, *Fiz. Tverd. Tela*, 1981, **23**, 975-982.
28. G. Jeschke, *Annu. Rev. Phys. Chem.*, 2012, **63**, 419-446.
29. B. E. Bode, D. Margraf, J. Plackmeyer, G. Durner, T. F. Prisner and O. Schiemann, *J. Am. Chem. Soc.*, 2007, **129**, 6736-6745.
30. P. E. Spindler, I. Waclawska, B. Endeward, J. Plackmeyer, C. Ziegler and T. F. Prisner, *J. Phys. Chem. Lett.*, 2015, **6**, 4331-4335.
31. A. Meyer, D. Abdullin, G. Schnakenburg and O. Schiemann, *Phys. Chem. Chem. Phys.*, 2016, **18**, 9262-9271.
32. A. Giannoulis, C. L. Motion, M. Oranges, M. Buhl, G. M. Smith and B. E. Bode, *Phys. Chem. Chem. Phys.*, 2018, **20**, 2151-2154.
33. D. Ulyanov, B. E. Bowler, G. R. Eaton and S. S. Eaton, *Biophys. J.*, 2008, **95**, 5306-5316.
34. A. J. Fielding, R. J. Usselman, N. Watmough, M. Slinkovic, F. E. Frerman, G. R. Eaton and S. S. Eaton, *J. Magn. Reson.*, 2008, **190**, 222-232.
35. S. Lyubenova, M. K. Siddiqui, M. J. M. P. de Vries, B. Ludwig and T. F. Prisner, *J. Phys. Chem. B*, 2007, **111**, 3839-3846.
36. K. Ackermann, C. Pliotas, S. Valera, J. H. Naismith and B. E. Bode, *Biophys. J.*, 2017, **113**, 1968-1978.
37. D. T. Edwards, T. Huber, S. Hussain, K. M. Stone, M. Kinnebrew, I. Kaminker, E. Matalon, M. S. Sherwin, D. Goldfarb and S. I. Han, *Structure*, 2014, **22**, 1677-1686.
38. A. Giannoulis, R. Ward, E. Branigan, J. H. Naismith and B. E. Bode, *Mol. Phys.*, 2013, **111**, 2845-2854.
39. G. Jeschke, M. Sajid, M. Schulte and A. Godt, *Phys. Chem. Chem. Phys.*, 2009, **11**, 6580-6591.
40. S. Valera, K. Ackermann, C. Pliotas, H. Huang, J. H. Naismith and B. E. Bode, *Chem. Eur. J.*, 2016, **22**, 4700-4703.
41. T. von Hagens, Y. Polyhach, M. Sajid, A. Godt and G. Jeschke, *Phys. Chem. Chem. Phys.*, 2013, **15**, 5854-5866.
42. A. Doll and G. Jeschke, *J. Magn. Reson.*, 2014, **246**, 18-26.
43. A. Doll and G. Jeschke, *J. Magn. Reson.*, 2017, **280**, 46-62.
44. A. Doll, S. Pribitzer, R. Tschaggelar and G. Jeschke, *J. Magn. Reson.*, 2013, **230**, 27-39.

45.   A. Doll, M. A. Qi, N. Wili, S. Pribitzer, A. Godt and G. Jeschke, *J. Magn. Reson.*, 2015, **259**, 153-162.
46.   P. E. Spindler, S. J. Glaser, T. E. Skinner and T. F. Prisner, *Angew. Chem. Int. Ed. Engl.*, 2013, **52**, 3425-3429.
47.   P. E. Spindler, P. Schops, W. Kallies, S. J. Glaser and T. F. Prisner, *J. Magn. Reson.*, 2017, **280**, 30-45.
48.   P. E. Spindler, Y. Zhang, B. Endeward, N. Gershernzon, T. E. Skinner, S. J. Glaser and T. F. Prisner, *J. Magn. Reson.*, 2012, **218**, 49-58.
49.   T. Bahrenberg, Y. Rosenski, R. Carmieli, K. Zibzener, M. Qi, V. Frydrnan, A. Godt, D. Goldfarb and A. Feintuch, *J. Magn. Reson.*, 2017, **283**, 1-13.
50.   B. Basel, MSc thesis, ETH Zürich, 2015.
51.   C. L. Motion, J. E. Lovett, S. Bell, S. L. Cassidy, P. A. S. Cruickshank, D. R. Bolton, R. I. Hunter, H. El Mkami, S. Van Doorslaer and G. M. Smith, *J. Phys. Chem. Lett.*, 2016, **7**, 1411-1415.
52.   E. Narr, A. Godt and G. Jeschke, *Angew. Chem. Int. Ed. Engl.*, 2002, **41**, 3907-3910.
53.   E. Narr, H. Zimmermann, A. Godt, D. Goldfarb and G. Jeschke, *Phys. Chem. Chem. Phys.*, 2003, **5**, 3959-3967.
54.   R. Hogg and R. G. Wilkins, *J. Chem. Soc.*, 1962, 341-350.
55.   K. Ackermann and B. E. Bode, *Mol. Phys.*, 2018, DOI: 10.1080/00268976.2017.1421324.
56.   M. Pannier, S. Veit, A. Godt, G. Jeschke and H. W. Spiess, *J. Magn. Reson.*, 2000, **142**, 331-340.